Korean J. Chem. Eng., **25**(2), 209-216 (2008)

Counter-current flow limitation velocity measured in annular narrow gaps formed between large diameter concentric pipes

Ji Hwan Jeong†

School of Mechanical Engineering, Pusan National University, Jangjeon-dong, Geumjeong-gu, Busan 609-735, Korea
(*Received 28 May 2007 • accepted 26 June 2007*)

Abstract−A two-phase flow configuration in which the gas phase flows upwards while the liquid phase flows downwards is referred to as a counter-current flow pattern. This flow configuration cannot be preserved if any flow rate exceeds a criterion known as the counter-current flow limitation (CCFL) or flooding. Since the CCFL is important to chemical engineers, it has long been studied via experimental and analytical approaches. Most of the previous CCFL experiments in annular channels have been carried out with a small diameter annulus and large gap-to-diameter ratio annulus. The present experiment examines the CCFL in narrow annular channels having gap sizes of 1, 2, 3, and 5 mm. The outer diameter of the annular passage is 500 mm. At a gap size of 1 mm, it was visually observed that a CCFL locally occurred in some region of the periphery while the other region remained in a counter-current flow configuration. The region under partial CCFL condition expanded with an increase in the air flow rate, finally reaching a global CCFL. The air flow rate for the global CCFL was roughly 15% larger than that for initiation of a partial CCFL. This difference in air flow rate between the initiation of a partial CCFL and the global CCFL was reduced as the gap size increased. When the gap size was 5 mm, the partial CCFL was not observed, but onset of flooding led to a global CCFL. Because of the existence of a transient period, the CCFL was experimentally defined as the situation where net water accumulation is sustained. The measured CCFL data are presented in the form of a Wallis' type correlation. Two length scales, hydraulic diameter and average circumference, were examined as the characteristic length scale. The average circumference appeared to better fit the experimental data, including results reported elsewhere. A new correlation using the average circumference as the characteristic length scale is suggested based on the experimental measurements of the present work and previous reports.

Key words: Flooding, CCFL, Annular Narrow Gap, Counter-current Flow, Characteristic Length

INTRODUCTION

Counter-current flow between two separate fluids is widely used in industries such as power plants and chemical process plants as this flow configuration gives maximum efficiency in heat and/or mass transfer between two phases. This flow structure cannot, however, be preserved by a limiting phenomenon known as CCFL or flooding. If either liquid or gas flow is supplied such that this criterion is exceeded, the flow pattern changes to a chaotic flow regime from a stable counter-current flow, and the fluids flow co-currently in the direction of the gas flow. As a consequence, the liquid phase cannot reach the plenum where the gas phase enters. The CCFL phenomenon has been of interest for chemical engineers since the 1930s because of its importance in designing chemical process plants such as wetted or packed column towers [1,2] and structured packings [3] wherein heat and mass transfer occur between gas and liquid phases. This phenomenon has also been of importance in the field of nuclear power plant (NPP) safety analysis [4].

In previous studies, the CCFL phenomenon in annular and rectangular gap geometries has been investigated in relation to nuclear power plants as well as chemical process plants. Specifically, the emergency core cooling water bypass [4], direct-vessel injection (DVI) [5], the safety margin of research reactor rectangular fuels [6-8], and postulated core melt accident [9] have been studied in this regard. Most analytical models and measured data on CCFL have been presented in terms of the Wallis parameter (j_k^*) or Kutateladze number (K_k^*) defined as follows:

$$j_k^* = j_k \sqrt{\frac{\rho_k}{gD(\rho_L - \rho_G)}}, \quad (1)$$

$$K_k^* = j_{k4} \sqrt{\frac{\rho_k^2}{g\sigma(\rho_L - \rho_G)}}, \quad (2)$$

where D, g, ρ, and σ represent the diameter as a characteristic length, the gravitational acceleration, the density, and the surface tension, respectively. The principal difference between these two dimensionless numbers is the choice of characteristic length. Wallis' parameter uses a test section geometry such as diameter, gap width and span, while the Kutateladze number uses the Taylor wave length. Thus, the Kutateladze number appears to be more adequate in terms of describing instability-induced phenomena such as CCFL. However, Wallis' parameter is still widely used by many researchers.

When selecting Wallis' parameter to describe CCFL models and fit their measurements, it is first necessary to decide what length scale to use. If the geometry of the test section is quite different from the circular pipe, there is no general guidance for the selection. Tables 1 and 2 list previous CCFL studies performed with rectangular and annular passages, respectively, as well as the sizes of the test sections used and the suggested correlations. In addition, the characteristic length scales used for the Wallis parameter are shown where applicable. For rectangular channels, various lengths have been used

†To whom correspondence should be addressed.
E-mail: jihwan@pusan.ac.kr

Table 1. Previous investigations on CCFL in rectangular passage

Author	W (cm)	S (cm)	L (cm)	Correlation	CL.
Cheng [6]	NA	NA	NA	$j_G^{*2}\left[W^{*2}j_G^{*2}+150+\frac{2W}{S}\right]+j_L^{*2}\left[(W^{*2}j_G^{*2}+150)\frac{W^{*4}j_G^{*4}}{4}\frac{\rho_G}{\rho_L}\frac{W^{*6}j_G^{*6}}{4}\right]$ $+j_G^{*}\lvert j_L^{*}\rvert\left[W^{*2}j_G^{*2}(W^{*2}j_G^{*2}+150)\sqrt{\frac{\rho_G}{\rho_L}}\right]=\frac{2}{3C_f}$, $W^{*}=2W/\lambda,\ \lambda=\sqrt{\sigma/(g\Delta\rho)}$	2W
Sudo and Kaminaga [8]	3.3 6.6	0.23 0.53 0.83 1.23	7.2 36.2 78.2	$j_G^{*1/2}+mj_L^{*1/2}=C$, $m=0.5+0.0015Bo^{1.3},\ C=0.66\left(\frac{S}{W}\right)^{-0.25},\ Bo=\frac{W\cdot S(\rho_L-\rho_G)g}{\sigma}$	S
Celata et al. [10]	15.0	0.2 0.5 1.0	30 12	$j_G^{*1/2}+j_L^{*1/2}=0.82,\ K_G^{*1/2}+1.6K_L^{*1/2}=1.2$	S
Osakabe and Kawasaki [11]	10.0	0.2 0.5 1.0	123.5	$j_G^{*1/2}+0.8j_L^{*1/2}=0.58$	W
Ruggles [12]	8.4	0.127	61.0	$j_G^{*1/2}+0.67j_L^{*1/2}=0.50$	W
Mishima [13]	4	0.15 0.24 0.50	47.0	$j_G^{*1/2}+j_L^{*1/2}=0.6$	2W
Lee [14]	NA	NA	NA	$j_G^{*1/2}+mj_L^{*1/2}=C$,* $m=0.5194+3.4019\left(\frac{S}{W}\right),\ C=0.6959+0.1618\log_{10}\left(\frac{S}{W}\right)$	2W

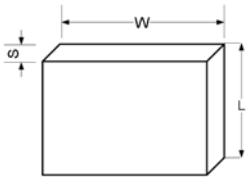

CL. characteristic length, W: channel span, S: gap size, L: length.
*Obtained by regression analysis for Mishima [13], Osakabe and Kawasaki [11] and Sudo and Kaminaga [8]'s experimental data.

as characteristic length scales to correlate measurements. Sudo and Kaminaga [8] and Celata et al. [10] used the gap width, S, while Osakabe and Kawasaki [11] and Ruggles [12] used the channel span, W, as the characteristic length. Cheng [6], Mishima [13], and Lee [14] suggested twice the span (2W) as the characteristic length scale. Similar suggestions have been made for annular passages. Richter et al. [15], Koizumi et al. [16], Ragland et al. [17] and Lee et al. [5] used the hydraulic diameter, which corresponds with twice the gap size (2S) for annular passages, while Richter [18], Osakabe and Kawasaki [11], and Nakamura et al. [19] used the average circumference of the annular passage (the circumference at the middle of an annulus) as the characteristic length scale. Richter et al. [15] measured CCFL points using a vertical annulus gap geometry whose gap size is 1 and 2 inches. They presented their measurements in terms of Wallis' parameters using the hydraulic diameter (D_h=2S) as a characteristic length scale. Their data were later correlated by Osakebe and Kawasaki [11] in terms of Wallis' parameter using the average circumference (W) as the characteristic length scale as follows:

$$j_G^{*1/2}+0.8j_L^{*1/2}=0.38. \quad (3)$$

It appears that many researchers select the characteristic length scale based on the best fit of data during the course of data regression rather than on the basis of theoretical considerations. Mishima [13] derived an analytical CCFL correlation and suggested using two times the gap size. In the present study, the selection of length measure for the characteristic length in the Wallis parameter is examined.

The sizes of the test sections listed in Tables 1 and 2 are compared in Fig. 1. Glaeser [20]'s facility is not compared in this plot since it is much larger than the others. This facility, known as the upper plenum test facility (UPTF), is of real nuclear reactor scale. The average circumference in Fig. 1 stands for the channel span of the rectangular passages and the circumference of the middle between the inner and outer walls of the annular passages. Most of the previous CCFL experiments involving annular passages were performed with small diameter (small average circumference) test sections. Furthermore, the gap sizes were relatively large. Typically, the outer diameter of the annular passage is smaller than 10 cm and the gap sizes are around 10 mm in the previous experiments. If a counter-current flow is developed in a test section of this size, the hydrodynamic phenomena would be quite uniform over the whole periphery, whereas it might show a 3-D effect in actual or large-sized test sections. Fig. 1 shows the geometries of the present facility. Compared with previous experimental facilities, the diameter of the present facility is large and the gap size is small. That is, the

Table 2. Previous investigations on CCFL in annular passage

Author	O.D. (cm)	I.D. (cm)	L (cm)	S (cm)	Correlation	CL.
Richter et al. [15]*	44.45	39.37	--	2.54	$j_G^{*1/2}+0.8j_L^{*1/2}=0.38$*	D_h
		34.29		5.08		W
Koizumi et al. [16]	10.0	9.9	50.0	0.05	$j_G^{*1/2}+0.23j_L^{*1/2}=0.32$ for 2 mm gap**	D_h
		9.8		0.1	$j_G^{*1/2}+0.35j_L^{*1/2}=0.35$ for 1 mm gap**	
		9.6		0.2		
		9.0		0.5		
Ragland et al. [17]	10.16	9.064	94.5	0.546	$j_G^{*1/2}+0.88j_L^{*1/2}=1.0$	D_h
Richter [18]	NA	NA	NA	NA	$C_wN_B^{3}j_G^{*6}S^{*2}j_L^{*2}+C_wN_B^{'}j_G^{*4}+150C_w\frac{j_G^{*2}}{S^*}=1$	W
Nakamura et al. [19]	22.0	20.0	--	1.0	$j_G^{*1/2}+0.78j_L^{*1/2}=0.37$***	W
Glaeser [20]	479	429	664	25.0	$K_G^{*1/2}\sqrt{\frac{v_G^{2/3}}{g^{1/3}l}}+0.011K_L^{*1/2}=0.0245$, $l=0.5\pi d_{outer}\sin^2(0.5\theta_{ECC\text{-}BCL})$	NA
McQuillan et al. [21]	6.0	3.8	27.8	1.1	$\frac{\zeta\sigma(D_a^2-D_r^2)}{4h^3}-\rho_Lg\left(\frac{\pi D_r}{2}+\frac{4h}{3}\right)+\frac{f_w\rho_LD_r}{h}\left(\frac{A}{A-A_r}\right)^2V_L^2=0$, $\sigma\zeta=h\Delta P$	NA
Roesler, Groll [22]	4.9	3.9	137	0.5	$2B_4f_i\delta^5(5f_i+\delta f_i^{'})(B_1^2-4B_4\delta^5f_i)^{-1/2}+(2f_i+\delta f_i^{'})[B_1+(B_1^2-4B_4\delta^5f_i)^{1/2}]=0$, $B_1=\frac{1}{\Delta h_G\rho_L\pi d_i}$, $B_4=-\frac{\rho_Lg}{3\rho_G\eta_L^2}\left(\frac{2}{\Delta h_G\pi d_i^2}\right)^2$	NA
Ueda, Suzuki [23]	2.8	1.0	100	0.9	$Fr=8.29\log_{10}X+19.18$,	NA
	3.5			1.25	$Fr=\sqrt{\frac{\rho_g(u_G+u_L)^2}{\rho_Lgy_i}}$, $X=\left(\frac{1}{Re_L}\right)^{1/3}\left(\frac{\rho_LgD_{eq}^2}{\sigma'}\right)^{1/4}\left(\frac{\eta_G}{\eta_L}\right)^{2/3}$	
	4.0			1.5		
Mishima [13]	NA	NA	NA	NA	$j_G^*-\frac{\varepsilon}{1-\varepsilon}\sqrt{\frac{\rho_G}{\rho_L}}j_L^*=\sqrt{\frac{\varepsilon^3(1-\varepsilon)}{3f_i}\left[1+\frac{3f_{wL}j_L^*\lvert j_L^*\rvert}{(1-\varepsilon)^3}\right]}$	2S

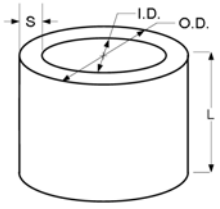

CL : characteristic length, W: average circumference, S: gap size, D_h: hydraulic diameter (=2S), L: length
*Richter et al. presented their measurements in terms of Wallis parameters using hydraulic diameter (D_h) as a CL and later Osakabe & Kawasaki [11] correlated them in terms of Wallis parameters using W as a CL.
** original data were presented in terms of Wallis parameters and correlated by Jeong et al. [24]
*** Original data were presented in terms of Wallis parameters and correlated by San Fabian et al. [25]

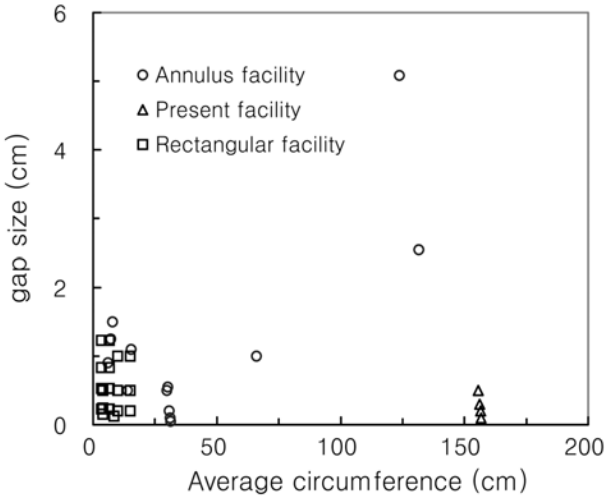

Fig. 1. Geometries of CCFL test facility of which passages are narrow gaps.

gap size to average circumference ratio of the present facility is much smaller than that of facilities considered in previous studies. Koizumi et al. [16] carried out an experimental study on CCFL in narrow annular passages. They measured flooding velocities in gap sizes ranging from 0.5 to 5 mm, which is nearly the same as the present gap size. However, the outer diameter of the annular passage was 10 cm, which is much smaller than that assessed here.

The effect of test section diameter associated with characteristic length scale in dimensionless numbers is not well understood at present. In this regard, it is necessary to carry out CCFL experiments in narrow annular passages with a large radius of curvature and make visual observations on flow behavior in a large diameter test section. The objectives of the present experiments are to visually observe the two-phase flow behavior inside a narrow annular gap and investigate the gap size effect on CCFL under large diameter conditions.

EXPERIMENTAL FACILITY

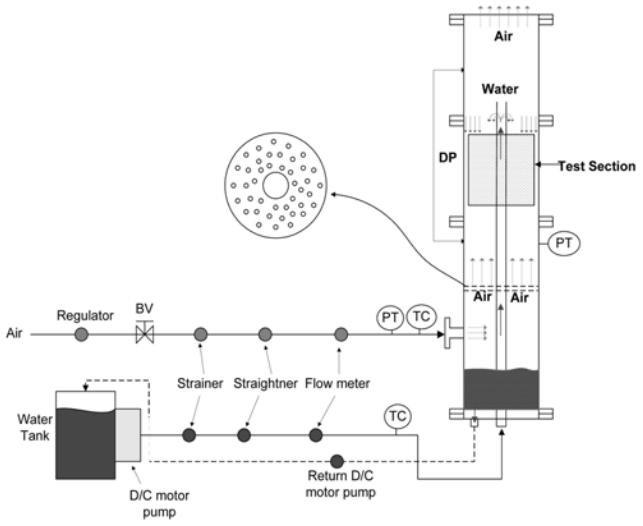

Fig. 2. Schematic diagram of the experimental facility.

The test rig was designed such that the water and air flows will be evenly distributed. A schematic diagram of the test facility is shown in Fig. 2. The test rig consists of a test section, a water reservoir, an air buffer tank, pumps & valves, pressure transducers, thermocouples, and turbine flow meters. Distilled water and air are used as working fluids. The high-pressure air coming out of the building supply line is provided to the flow control valve and turbine flow meter via an air filter and an air buffer tank whose volume is 1.3 cubic meters. The air buffer tank is used in order to damp down air pressure fluctuation and make a smooth change of air flow. Metered air is introduced to the lower plenum of the test section, and travels up through a multi-holed plate that is used to achieve an evenly distributed flow velocity. The water in the reservoir is forced to flow by a controllable DC pump, and the flow-rate is measured by a turbine flow meter. The water is supplied to the upper part of the test section through holes made on the central pole. The central pole serves as a water supply line as well as an alignment axis for the test section. The water proceeding down to the lower plenum returns to the water reservoir by a pump. The water circulates in a closed loop, and the air is discharged into the atmosphere. A cooling coil is installed inside the water reservoir to maintain the water temperature at a constant level. The cooling coil eliminates the heat generated by the pump. Measurements are made on the differential pressure across the test section, system pressure, air-line pressure, air flow rate, and supplied water flow rates. All signals from the sensors are read by an HP-VXI data acquisition system, and graphically displayed on a PC-monitor as well as saved on a hard disk.

The components of the test section are made of acrylic resin so as to allow visual observation on the two-phase flow behavior inside the gaps. The inner diameter of the outer pipe, which forms the annular passage, and the length of the inner cylinder are 500 and 250 mm, respectively. Gap sizes of 1, 2, 3, and 5 mm were established by utilizing various inner cylinder diameters. Although most parts of the test section were machined by a computer numerical control (CNC) lathe, the gap sizes may not be uniform due to manufacturing tolerance. For instance, a gap size of 1 mm is too small compared with the diameter of the outer pipe of 500 mm. A manufacturing tolerance of 0.1% causes a deviation of ±0.25 mm in the gap size, which corresponds to 25% variation for a 1 mm gap.

In general, three kinds of errors must be considered in order to quantify the error bound of the CCFL velocity measurements: inherent error of the instruments, reading error, and systematic error that is introduced due to experimental procedure. In the present experiment, there is a systematic error arising from the difference between the estimated and actual CCFL velocities, since the air flow rate was step-wisely increased until the CCFL occurred. The flowmeters used in these experiments are accurate within 1% and the signal transducer can read the signal within 1% errors. If we assume the systematic error is less than 10% of the exact value, the maximum error for reading the volume flow rate (Q_k) is

$$\Delta Q_k=(1.01\times1.01\times1.1-1)Q_k=0.122Q_k.$$

In addition, one more source of error should be considered in the present experiment, the error due to test section manufacturing tolerance. As noted earlier, manufacturing tolerance can cause variation of gap size. This gap size uncertainty contributes to error in the superficial velocity ($j_k=Q_k/A$). When the inaccuracy of each parameter is known, the error bound of the computed result can be estimated by the method of error propagation based on Taylor series expansion. According to this method, the error in the Wallis parameter is about 27%. The gap size uncertainty makes the largest contribution to the error bound.

PROCEDURES AND CCFL DEFINITION

Since the air and water inlet conditions may have a considerable effect on the onset of CCFL, care was taken to confirm that both flows were well distributed. Whenever the test section was changed and reassembled, the air flow distribution was confirmed by using anemometers without a water supply. After the air flow distribution was confirmed, the water was supplied to a predetermined level. The minimum water flow rate tested in the experiments was large enough to cover the whole water inlet surface. In other words, the tested water flow rate was larger than a water flow rate that would develop rivulets at the water inlet. After the water flow developed at the water inlet, the water depth on the top of the test section was measured to confirm that the water flow was evenly distributed along the whole circumference of the annular channel inlet. After confirming even distribution of the water supply, we increased the air flow-rate step-wise. At each level of air flow-rate, the two-phase flow behavior inside the gap and water accumulation in the upper plenum was observed with the naked eye. The pressure difference between the top and the bottom of a gap was also monitored. Both air and water flow-rates were not altered and were observed for more than 10 minutes. If there was no sign of water accumulation in the upper plenum, the air flow-rate was increased further. This process was repeated until a significant increase in the differential pressure across the gap was obtained and water started to accumulate in the upper plenum. These two indicators, water accumulation and a significant increase in the differential pressure, are used as an experimental definition of the occurrence of CCFL in the present study. This definition has been generally accepted in previous reports. Even if CCFL locally occurs in a part of the gap, the point where there is no water accumulation in the upper plenum is not considered as

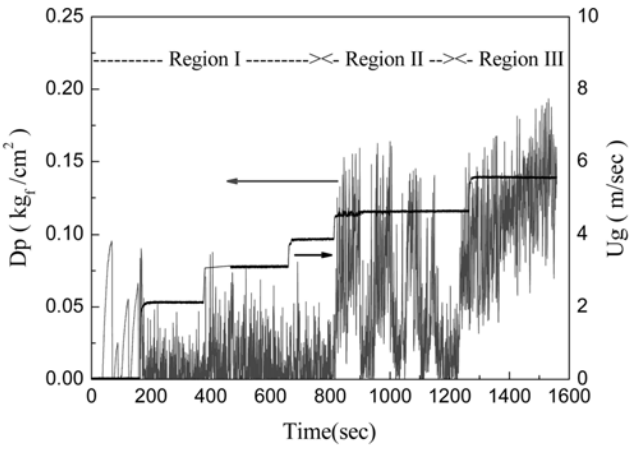

Fig. 3. Pressure difference between the top and the bottom of a 1 mm wide annular passage ($j_L^{*1/2}$=1.152).

the CCFL. This is because this condition is not problematic from the viewpoint of a nuclear safety analysis. Regardless, all the supplied water penetrates gaps and reaches the lower plenum. Further observations are described in the following section.

RESULTS AND DISCUSSIONS

1. Visual Observations

Each run started with fixing a liquid phase flow rate at a pre-determined value. The air flow-rate was step-wise increased from zero while the liquid flow rate was fixed at a pre-set value. The pressure difference between the top and the bottom of the annular gap was monitored. In addition, the behavior of water and air inside a narrow annular gap was visually observed, and images were captured with a camera. Fig. 3 shows a trace of the differential pressure for a test section having a gap size of 1 mm. The water supply was fixed at $j_L^{*1/2}$=1.152. The somewhat long trace before time zero shown in Fig. 3 was truncated to give a clear figure around the onset of CCFL. The trace can be divided into three regions. Region I covers up to 800 seconds in Fig. 3. A dozen stepwise increases in air flow-rate were made before 800 seconds. Through this period, the water supplied to the upper plenum penetrated the annular gap and hence no accumulation of water was observed in the upper-plenum. The pressure difference across the annular passage fluctuated within a limited range. Region II extends from the end of region I to 1,200 seconds. The air flow rate increased slightly at 800 seconds. The water supplied into the upper-plenum started to accumulate. Water accumulation did not continue over a period of roughly two minutes, but penetrated the gap until no accumulated water remained in the upper-plenum. After approximately a minute, the water started to accumulate again. That is, the water in the upper plenum showed cyclic behavior of accumulation and penetration. This cyclic behavior continued until the air flow rate increased up to just below the value of CCFL. Through this region, the pressure difference between the top and the bottom of the annular passage increased and dropped in accordance with the cyclic behavior of the water. The pressure difference increased as water accumulated, and decreased as the water penetrated. However, if the air flow was increased just slightly beyond than that of the CCFL criterion, the water accumulation continued and did not show cyclic behavior. This is region III. The average pressure difference continued to increase as the accumulation height increased in this region.

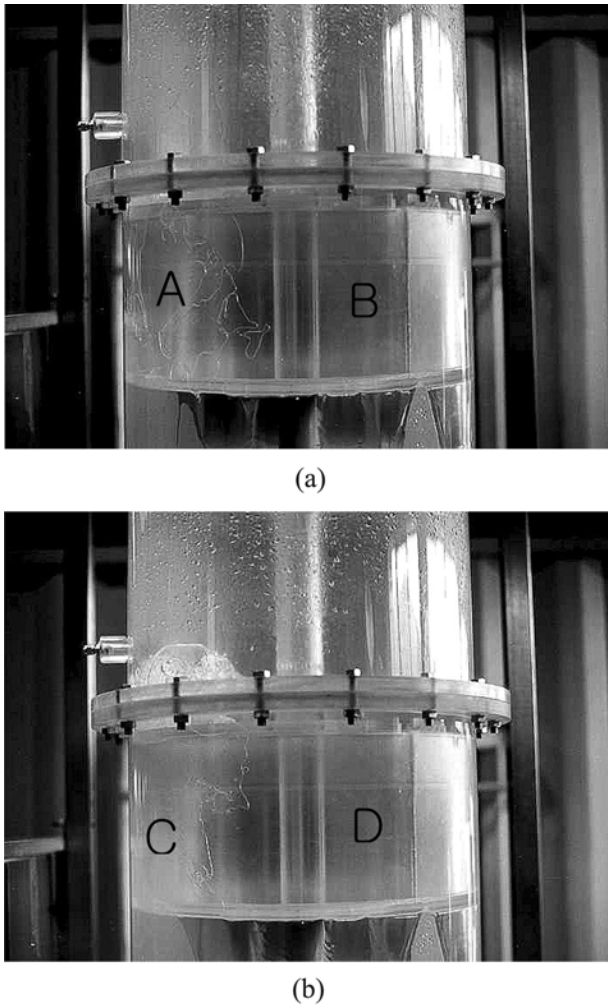

Fig. 4. Partially limiting CCFL (1 mm gap, $j_L^{*1/2}$=1.152).

It was visually observed that the flow behavior inside gaps was not uniform, as shown in Fig. 4. The image in Fig. 4(b) was taken 100s after that in Fig. 4(a) had been taken. These photographs show typical flow behavior in region II. When the air flow is increased up to region II, partial CCFL initiates at the top of the annular gap. There are two distinct regions, denoted as "A" and "B" in Fig. 4(a) and "C" and "D" in Fig. 4(b). Region "A" has many irregular lines, which are the air-water interface. This irregular air-water interface implies that the counter-current flow pattern is not preserved but changed into a churn flow pattern. Region "C" of Fig. 4(b) shows no liquid film. An upward co-current flow is configured in this region. Also, we can see a water bump on the top of region "C", which is a water eruption caused by upward air flow. This region appears to be under CCFL. At the same time, regions "B" and "D" appear transparent. No irregular air-water interfaces are seen. The region still preserves a counter-current flow pattern. That is, some parts of the annular gap are under CCFL conditions, and other parts remain in a counter-current flow pattern. This indicates that water is prevented from penetrating some part of the gap while it is allowed to flow

downwards at other parts. The CCFL limited region expands with an increase in the air flow rate. Through a set of experimental runs, it was observed that CCFL always is initiated in the same part of the gap. This appears to be attributable to the manufacturing tolerance of the rig.

The components of the test section are made of acrylic resin so as to allow visual observation of the two-phase flow behavior inside gaps. A thick resin pipe was machined by a CNC lathe in order to fabricate the parts of the test section. A machining tolerance of ±0.1% produces a variation of ±0.25 mm in gap size for the present test section of which the diameter is 500 mm. The intended gap size of 1 mm may vary from 0.75 to 1.25 mm, which corresponds to ±25% deviation. For a 2 mm gap, the deviation could be 12.5%. This is a large deviation relative to the gap size of 1 mm. Despite the fact that water cannot penetrate the gap at some part of the periphery due to local CCFL, this air velocity is not defined as the CCFL gas velocity. This is because all the water supplied to the upper plenum penetrates the gap and proceeds to the lower plenum through the other part of the gap.

If the air flow rate is increased further, the flow configuration advances to region III. At this air flow rate, the whole periphery falls under CCFL as shown in Fig. 5(a). These pictures show no downward water flow in the gap, but we can see a thin water film is sheared by upward air flow (region A). Also, we can see repeated water bumps (noted by "B") developing on the top of the gap in a somewhat regular pattern. In some cases, however, accumulated water penetrates a part of the gap, as shown in Fig. 5(b). The region, designated by "C", shows penetrating water. In the same image, CCFL is preserved in region "D". This penetration lasts for a period of time, and then ends. Even though temporary penetration occurs, water accumulation in the upper-plenum still continues. Based on these observations, the CCFL is defined in the present work as the situation where net water accumulation is sustained.

The description given above is for a 1 mm gap case. For this case, the CCFL gas velocity was roughly 15% larger than the gas velocity for the initiation partial occurrence of CCFL (region II). It should be noted that the air velocity for the initiation of partial CCFL increased as the gap size increased. Thus, the difference in air velocities between the initiation of partial CCFL and global CCFL is reduced as the gap size is increased. At a gap size of 5 mm, the difference was difficult to discern.

2. CCFL Measurements

Fig. 6 shows the present measurements for 1, 2, 3, and 5 mm gaps in terms of Wallis' parameter. The gap size (S) is used as the characteristic length scale in this plot. Gap sizes of the present facility, i.e., 1, 2, 3, and 5 mm, are less than the wavelength of Taylor instability, 17.2 mm, as defined by $\lambda_T=2\pi\sqrt{\sigma/g\Delta\rho}$. The average circumference of the present facility, around 1,570 mm, is much larger than the Taylor wavelength. The ratio of gap size to average circumference is roughly 0.4-2% for the present facility. Compared with the gap size, the circumferential length is so large that it can be assumed to be infinite. Therefore, the average circumference may not be appropriate to serve as the characteristic length scale with respect to taking the effect of gap size into account. In this regard, measurements plotted in Fig. 6 are expressed in terms of Wallis' parameters with a characteristic length scale of the gap size. The Richter et al. [15] and Koizumi et al. [16] measurements are also plotted here. Both researchers used the hydraulic diameter (D_h) as the character-

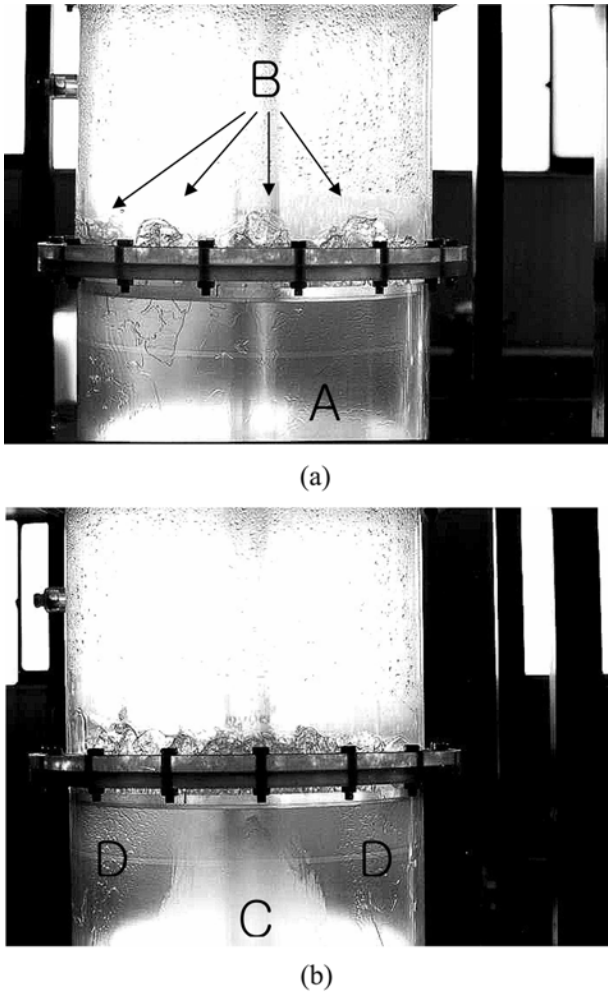

Fig. 5. Fully limiting CCFL (1 mm gap, $j_L^{*1/2}$=1.152).

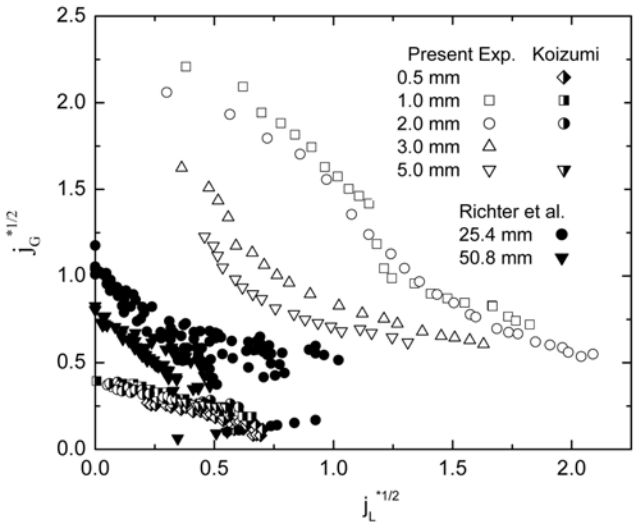

Fig. 6. CCFL points in Wallis' parameter with gap size (=D_h/2) as characteristic length.

istic length scale to present their measurements in the original reports. The test section of Richter et al. [15] consists of an outer tube whose I.D. is 17.5 in (44.45 cm) and a inner tube whose O.D. is 15.5 in (39.37 cm) and 13.5 in (34.29 cm) to produce 1 in (2.54 cm) and 2 in (5.08 cm) gaps, respectively. In the test section of Richter et al. the outer diameter is close to the present one, i.e., 500 mm. In terms of gap size, however, the present test section is much smaller than that of Richter et al. The gap sizes of the Koizumi et al. [16] test section vary from 0.5 mm to 5 mm, roughly corresponding to the gap size of the present test section. However, the outer diameter of the annular passage of the Koizumi et al. test section is 10 cm, which is much smaller than the present case. Fig. 6 shows the general tendency in variation depending on gap size. The CCFL points become larger as the gap size decreases. However, CCFL data in this plot are grouped such that there may be another factor influencing the CCFL points. The present data are much larger than the Koizumi et al. data even though the gap sizes are nearly the same. On the contrary, the Richter et al. data are closer to the present data in spite of a large difference in gap size. As noted previously, Koizumi et al.'s test section has a significantly different radius from the present experiments while the radius of Richter et al.'s test section is very close to that of the present experiments. This implies that the influence of diameter (D) or averge circumference (W=π(I.D.+O.D.)/2) of the annular channel needs to be considered.

All data presented in Fig. 6 are transformed into a Wallis parameter byusing the average circumference as the characteristic length scale, and plotted in Fig. 7. Richter et al.'s data appear to be similar to the present data even though the difference in gap size is large. Koizumi et al.'s data appear to be apart from the present data even if there is little difference in the gap size. However, these three data sets are placed in order of average circumference. The average circumference of the present data, Richter et al.'s data, and Koizumi et al.'s data are 156.8-155.5, 131.7-123.7, and 31.3-29.8 cm, respectively. The average circumference of Richter et al. and Koizumi et al.'s facility corresponds to 84% and 20% of the present test facility, respectively. Figs. 6 and 7 show that the average circumference appears to be more appropriate than the gap size or hydraulic diameter to present or correlate CCFL data gathered by using annular passages.

The measurements shown in Fig. 7 are correlated in the form of Eq. (4).

$$j_G^{*1/2} + m j_L^{*1/2} = C \tag{4}$$

where $j_k^* = j_k \sqrt{\dfrac{\rho_k}{gW(\rho_L - \rho_G)}}$.

It should be noted that "D" in Eq. (1) is exchanged with "W" in the above equation. As stated above, the average circumference is used as the characteristic length scale. In order to use this length scale in determining the constants m and C, a ratio of the average circumference to the Taylor wavelength is considered. This ratio reduces to a bond number, N_B, whose relation is as follows:

$$\frac{W}{\lambda_T} = \sqrt{\frac{W^2 g \Delta\rho}{\sigma}} = \sqrt{N_B}. \tag{5}$$

The constants m and C are fitted by the least-square method as follows:

$$m = -1.60 + 0.43 \log_{10} N_B \tag{6}$$

$$C = -0.78 + 0.21 \log_{10} N_B. \tag{7}$$

These expressions show that the constants m and C increase with an increase in average circumference. The predictions by Eq. (4) for the present, Richter et al.'s, and Koizumi et al.'s data are presented in Fig. 7. This plot shows a good agreement between the measured data and Eq. (4) through (7). Fig. 8 presents a quantative comparison between the CCFL gas velocity experimental data and Eq. (4): the absolute percentage deviation is around 10%.

CONCLUDING REMARKS

The counter-current flow limitation in narrow annular passages having a large diameter of curvature has been investigated. The principal difference between the present and previous facilities providing an annular passage is the small gap size compared with the radius of curvature. The tested gap sizes were 1, 2, 3 and 5 mm. This gap size is very small compared with the outer diameter of the annular

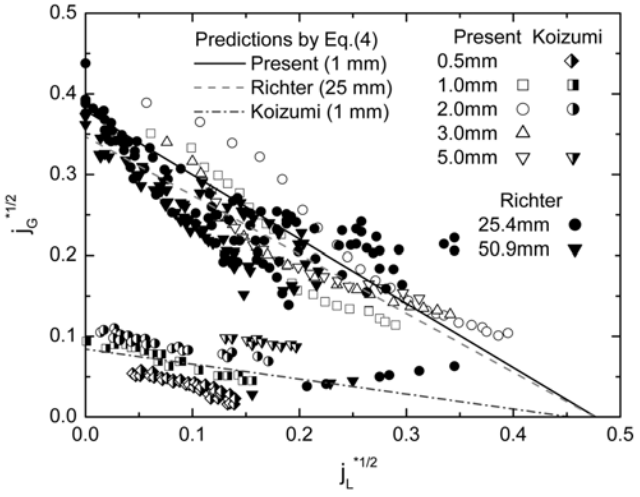

Fig. 7. CCFL points in Wallis' parameter with average circumference as characteristic length.

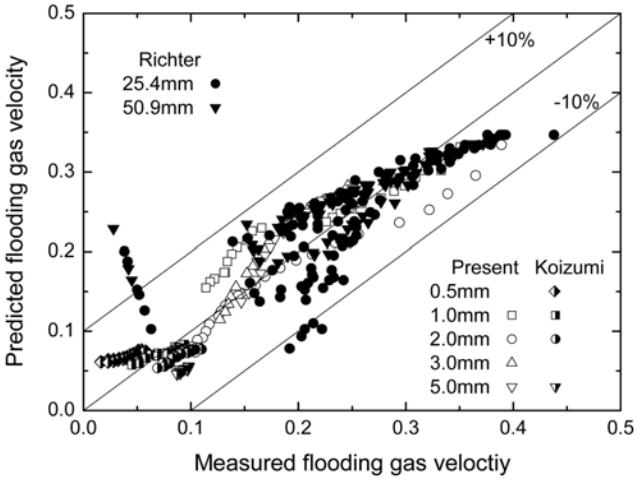

Fig. 8. Predicted vs. measured gas velocity at CCFL.

passage, i.e., 500 mm. It was visually observed that a CCFL might locally occur in some part of the periphery while the other parts remain in a counter-current flow regime. Although water cannot penetrate the gap at some parts of the periphery due to local CCFL, this air velocity is not defined as the CCFL gas velocity. This is because the water supplied to the upper plenum penetrates the gap and travels down to the lower plenum through another part of the gap. Based on these observations, CCFL is defined in the present work as the situation where net water accumulation is sustained. Comparison of the present and previous experimental data reveals that average circumference is more appropriate than the gap size or hydraulic diameter to correlate the CCFL data obtained from annular passages having large diameter regardless of gap size. An empirical correlation in terms of Wallis' parameter was developed by means of the least-squares method from the measured data. The average circumference was used as the characteristic length, and the results show that the absolute value of the slope and the y-intercept of the Wallis type CCFL correlation increase with an increase in average circumference.

ACKNOWLEDGEMENT

This work was supported by the Basic Atomic Energy Research Institute (BAERI) and Korea Foundation for International Cooperation of Science & Technology (KICOS) through a grant provided by the Korean Ministry of Science & Technology (MOST) in 2007.

NOMENCLATURE

C : constant
D : diameter
D_h : hydraulic diameter
f : friction coefficient
g : gravitational acceleration
j_k : non-dimensional superficial velocity of *k*-phase
j_k^* : Wallis' parameter $(j_k\sqrt{\rho_k/gD(\rho_f-\rho_g)})$
K_k^* : Kutateladze number $(j_k\sqrt{\rho_k^2/g\sigma(\rho_f-\rho_g)})$
L : length
m : constant
N_B : Bond number $((W/\lambda_T)^2)$
P : pressure
S : gap size
u : velocity
W : average circumference

Greek Letters

ε : average volume fraction
δ : film thickness
λ_T : Taylor wavelength
ρ : density
σ : surface tension

Subscripts

g : gas phase
f : liquid phase
i : interface
w : wall

REFERENCES

1. H. Imura, H. Kusuda and S. Funatsu, *Chemical Engineering Science*, **32**, 79 (1977).
2. D. H. Han and W. H. Hong, *Korean J. Chem. Eng.*, **15**, 324 (1998).
3. S. Y. Cho, Y. Y. Lee and S. J. Kim, *Korean J. Chem. Eng.*, **12**, 313 (1995).
4. F. Mayinger, P. Weiss and K. Wolfert, *Nucl. Eng. & Des.*, **145**, 47 (1993).
5. S. C. Lee, C. Mo, S. C. Nam and J. Y. Lee, *Thermal-hydraulic behaviours and flooding of ECC in DVI systems*, KAERI/CM-045/95, KAERI (1995).
6. L. Y. Cheng, *Counter-current flow limitation in thin rectangular channels*, BNL-44836, BNL (1990).
7. K. Mishima and H. Nishihara, *Nucl. Eng. & Des.*, **86**, 165 (1985).
8. Y. Sudo and M. Kaminaga, *Int. J. Multiphase Flow*, **15**, 755 (1989).
9. J. H. Jeong, S. J. Lee, R. J Park and S. B. Kim, *J. of Korean Nuclear Society*, **34(4)**, 396 (2002).
10. G. P. Celata, G. E. Farello, M. Furrer and M. Cumo, *Flooding experiments in a rectangular geometry*, RT/TERM/85/3, ENEA (1985).
11. M. Osakabe and Y. Kawasaki, *Int. J. Multiphase Flow*, **15**, 747 (1989).
12. A. E. Ruggles, *Countercurrent flow limited heat flux in the high flux isotope reactor (HFIR) fuel element*, ORNL/TM-9662, ORNL (1990).
13. K. Mishima, *Boiling burnout at low flow rate and low pressure conditions*, Ph.D. Thesis, Kyoto Univ. (1984).
14. S. Y. Lee, *Nuclear Technology*, **104**, 64 (1993).
15. H. J. Richter, G. B. Wallis and M. S. Speers, *Effect of scale on two-phase countercurrent flow flooding*, NUREG/CR-0312, NRC (1979).
16. Y. Koizumi, H. Nishida, H. Ohtake and T. Miyashita, *Proceedings of NURETH-8*, **1**, 48 (1997).
17. W. A. Ragland, W. J. Minkowycz and D. M. France, *Int. J. Heat and Fluid Flow*, **10**(2), 103 (1989).
18. H. J. Richter, *Int. J. Multiphase Flow*, **7**, 647 (1981).
19. H. Nakamura, Y. Koizumi, Y. Anoda and K. Tasaka, *Proceedings of 27th National Heat Transfer Symposium of Japan*, 964 (1990).
20. H. Glaeser, *Nucl. Eng. & Des.*, **133**, 259 (1992).
21. K. W. McQuillan, P. B. Whalley and G. F. Hewitt, *Int. J. Multiphase Flow*, **11**(6), 741 (1985).
22. S. Roesler and M. Groll, *Proc. of 1991 National Heat Transfer Conference*, Minnesota, 91 (1991).
23. T. Ueda and S. Suzuki, *Int. J. Multiphase Flow*, **4**, 157 (1978).
24. J. H. Jeong, R. J. Park and S. B. Kim, *Heat and Mass Transfer*, **34**, 321 (1998).
25. J. San Fabian, J. Guilleme, U. Hansen, M. Osakabe and H. Futamata, *Int. J. Multiphase Flow*, **22**(5), 883 (1996).